

Diagnostic of chemical abundances and ages from the line strength indices H_β , $\langle\text{Fe}\rangle$, and Mg_2 : what do they really imply ?

R. Tantaló¹, A. Bressan², C. Chiosi¹

¹ Department of Astronomy, Vicolo dell' Osservatorio 5, 35122 Padua, Italy

² Astronomical Observatory, Vicolo dell' Osservatorio 5, 35122 Padua, Italy

Received: April 1997. Accepted:

Abstract. The line strength indices H_β , Mg_2 , and $\langle\text{Fe}\rangle$, together with their gradients and dependence on the galaxy luminosity (mass), observed in elliptical galaxies are customarily considered as reliable indicators of systematic differences in age and abundances of Mg and Fe. Furthermore, as the gradient in Mg_2 happens to be often steeper than the gradient in $\langle\text{Fe}\rangle$, an enhancement of Mg (α -elements in general) with respect to Fe toward the center of these systems or going from dwarf to massive ellipticals is inferred. In this paper, we address the question whether or not the indices Mg_2 and $\langle\text{Fe}\rangle$ (and their gradients) are real indicators of chemical abundances and enhancement of these or other effects must be taken into account. We show that this is not the case because the above indices are severely affected by the *unknown* relative percentage of stars as function of the metallicity. In order to cast the problem in a fully self-consistent manner, first we provide basic calibrations for the variations δH_β , δMg_2 , and $\delta \langle\text{Fe}\rangle$ as a function of the age $\Delta \log(t)$ (in Gyr), metallicity $\Delta \log(Z/Z_\odot)$, and $\Delta[\text{Mg}/\text{Fe}]$. Second and limited to three elliptical galaxies of the Carollo & Danziger (1994a) catalog, we analyze the implications of the gradients in Mg_2 and $\langle\text{Fe}\rangle$ observed across these systems. It is shown from a quantitative point of view how the difference δMg_2 and $\delta \langle\text{Fe}\rangle$ between the local (radial distance r) and central values of each index would translate into difference $\Delta[\text{Mg}/\text{Fe}]$, $\Delta \log(Z/Z_\odot)$, and $\Delta \log(t)$. Finally, the above calibration is used to explore the variations from galaxy to galaxy of the nuclear values of H_β , Mg_2 , and $\langle\text{Fe}\rangle$ limited to a sub-sample of the Gonzales (1993) catalog. The differences δH_β , δMg_2 , and $\delta \langle\text{Fe}\rangle$ are converted to differences $\Delta \log(t)$, $\Delta \log(Z/Z_\odot)$, and $\Delta[\text{Mg}/\text{Fe}]$. Various correlations among the age, metallicity, and enhancement variations are explored. In particular, we thoroughly examine the relationship $\Delta \log(t) - M_V$, $\Delta \log(Z/Z_\odot) - M_V$, and $\Delta[\text{Mg}/\text{Fe}] - M_V$, and advance the suggestion that

the duration of the star forming period gets longer or the age of the last episode of stellar activity gets closer to the present at decreasing galaxy mass. This result is discussed in the context of current theories of galaxy formation and evolution. i.e. merger and isolation. In brief, we conclude that none of these can explain the results of our analysis, and suggest that the kind of time and space dependent IMF proposed by Padoan et al. (1997) and the associated models of elliptical galaxies elaborated by Chiosi et al. (1997) should be at work.

Key words: Galaxies: chemical abundances – Galaxies: line strength indices – Galaxies: stellar content – Galaxies: ellipticals

1. Introduction

The line strength indices H_β , Mg_2 , and $\langle\text{Fe}\rangle$ and their gradients are considered as good indicators of age and metallicity and customarily used either to infer these important physical quantities in specific regions of galaxies (the nucleus for instance), or to derive the age and composition (abundances of Mg and Fe) gradients across these systems. Elliptical galaxies are the most popular targets of these studies. In addition to this, since the gradients in Mg_2 and $\langle\text{Fe}\rangle$ (Carollo & Danziger 1994a,b; Carollo et al. 1993) observed in elliptical galaxies have different slopes arguments are given for an enhancement of Mg (α -elements in general) with respect to Fe toward the center of these galaxies. Finally, the inferred degree of enhancement seems to increase passing from dwarfs to massive ellipticals (see Worthey et al. 1994, Faber et al. 1992, and Matteucci 1997 for recent reviews of all these subjects and exhaustive referencing).

That H_β correlates with the age is not a surprise, because this index is known to be most sensitive to the light

Send offprint requests to: R. Tantaló

emitted by stars at the turnoff. However, since the properties of these latter also depend on the chemical composition, we expect H_β to be affected by chemical parameters as well in a way that must be ascertained a priori in a self-consistent fashion.

The bottom line to infer from Mg_2 and $\langle Fe \rangle$ an enhancement in α -elements rests on the implicit notion that these two indices strongly depend on the metallicity in general and on the abundances of Mg and Fe in particular and very little on the age. If this is the case, as Fe is mainly produced by Type Ia supernovae (accreting white dwarfs in binary systems) and in smaller quantities by Type II supernovae, the iron abundance $[Fe/H]$ continuously increases as the galaxy ages. In contrast only Type II supernovae contribute to oxygen and α -elements. Recalling that the mean lifetime of a binary system (Type Ia progenitors) is ≥ 1 Gyr, the $[\alpha/Fe]$ ratios are expected to decrease during the galaxy evolution. This means that to obtain a galaxy (or region of it) enhanced in α -elements the time scale of star formation over there must be shorter than about 1 Gyr. This is a very demanding constraint on models of galaxy formation and evolution.

In this paper, we address the question whether or not the indices Mg_2 and $\langle Fe \rangle$ (and their gradients) are real indicators of chemical abundances and abundance ratios or other subtle effects must be taken into account. More specifically, using the spherical models of elliptical galaxies with gradients of mass density, star formation rate, and chemical abundances developed by Tantalo et al. (1997) for which the chemical abundances are known as a function of time and radial distance, we check how gradients in Mg and Fe (and their ratio) translate into gradients in Mg_2 and $\langle Fe \rangle$, and check whether a gradient in Mg_2 steeper than the gradient in $\langle Fe \rangle$ implies an enhancement of the Mg with respect to Fe toward the center of these galaxies. We anticipate here that, while these models are indeed able to match many key properties of elliptical galaxies, including the gradients in broad band colors (see below), they lead to contradictory results as far as the gradients in line strength indices are concerned (section 2). To understand the physical cause of this odd behaviour of the models, we check the calibration in use and the response of Mg_2 to chemistry (section 3). The reason of the contradiction is found to reside in the heavy dependence of the indices in question on the metallicity distribution function $N(Z)$ of the stellar populations in a galaxy. In addition to this, the observed gradients in the indices Mg_2 and $\langle Fe \rangle$ in particular, do not automatically correspond to gradients in the Mg and Fe abundances (section 3). In order to tackle the whole problem in a fully self-consistent way we derive new basic relationships providing the variation of the line strength indices H_β , Mg_2 , and $\langle Fe \rangle$ of single stellar populations (from which eventually the galactic indices are built up) as a function of age t , total metallicity Z , and $[Mg/Fe]$ (section 4). The analysis is made for a few test galaxy of the Carollo & Danziger (1994a,b) sam-

ple. Second, we apply the above diagnostic to study the observational variations of nuclear values of H_β , Mg_2 and $\langle Fe \rangle$ from galaxy to galaxy of the Gonzales (1993) sample and translate these variations into differences in age, metallicity, and enhancement of α -elements (section 5). A preliminary ranking of galaxies as a function of their last episode of star formation is attempted (section 6). The results of the analysis are discussed at the light of the present-day understanding of the mechanism of formation and evolution of elliptical galaxies: i.e. isolation or merger (section 7), and the SN-driven galactic wind or variable IMF schemes (section 8). Finally, some concluding remarks are drawn (section 9).

2. The reference model

2.1. The basic assumptions

Elliptical galaxies are described as spherically symmetric systems whose mass density decreases outward. The density of luminous material as a function of the radial distance and the corresponding gravitational potential are derived from Young (1976). We assume that each shell contains about 5% of the total mass in the luminous material M_L . The mass distribution and gravitational potential of the dark-matter as a function of the radial distance are derived from the density profile of Bertin et al. (1992) however adapted to the Young formalism. The total mass M_D and radius R_D of the dark-matter component are assumed to be $5 \times M_L$ and $5 \times R_L$, respectively.

In order to simulate the collapse of luminous material into the potential well of dark-matter (whose mass is assumed to be constant in time) the infall scheme is adopted and the density of luminous material (gas) is let grow with time at the rate:

$$\frac{d\rho_L(r,t)}{dt} = \rho_{L0}(r)e^{-\frac{t}{\tau(r)}} \quad (1)$$

where $\tau(r)$ is the time scale of gas accretion (in principle it can be a function of the radial distance), and $\rho_{L0}(r)$ is fixed by imposing that at the present-day age of the galaxy T_G the density of luminous material in each shell has grown to the value given by the Young profile.

A successful description of the gas accretion phase is possible adapting to galaxies the radial velocity law describing the final collapse of the core in a massive star, i.e. free-fall in all regions external to a certain value of the radius ($v(r) \propto r^{-\frac{1}{2}}$) and homology inside ($v(r) \propto r$). This picture is also confirmed by numerical calculations of dynamical models with the Tree-SPH technique (cf. Carraro et al. 1997). This simple scheme allows us to derive the radial dependence of $\tau(r)$ as a function of some arbitrary time scale. For this latter we adopt the mean free-fall time scale of Arimoto & Yoshii (1987).

The rate of star formation (SFR) follows the standard Schmidt law

$$\Psi(r,t) = \nu(r)\rho_{Lg}(r,t) \quad (2)$$

where $\rho_{Lg}(r, t)$ is the local gas density and $\nu(r)$ is the specific efficiency. For this latter, we have adopted the formulation by Arimoto & Yoshii (1987).

The chemical evolution of elemental species is governed by the same set of equations as in Tantaló et al. (1996) however adapted to the density formalism and improved as far as the ejecta and the contribution from Type Ia and Type II supernovae are concerned according to the revision made by Portinari et al. (1997) to whom we refer.

The models allow for galactic winds triggered by the energy deposit from Type I and II supernova explosions and stellar winds from massive stars. To evaluate the amount of energy stored into the interstellar medium by supernova explosions we adopt the same cooling law as in Gibson (1994, 1996).

Finally, the line strength indices Mg_2 and $\langle Fe \rangle$ have been calculated adopting the calibrations by Worthey (1992) and Worthey et al. (1994) as a function of $[Fe/H]$, T_{eff} and gravity of the stars.

The basic data for the two innermost shells of a typical galaxy with total luminous mass $3 \times 10^{12} M_{\odot}$ are given in Table 1, whereas the evolution of a few chemical abundances limited to the central region ($r = 0.06 R_e$) is shown in Fig. 2. The content of Table 1 is as follows: $M_{L,12}$ is the asymptotic luminous mass in units of $10^{12} M_{\odot}$; ν is the efficiency of the SFR; τ is the time scale of gas accretion in Gyr; Z_{max} and $\langle Z \rangle$ are the maximum and mean metallicity, respectively; $G(t)$ and $S(t)$ are the fractionary gas and alive star densities, respectively (both are normalized to the asymptotic mass $M_{L,12}$); N_{enh} is the percentage of α -enhanced stars present in the model (see below).

These galactic models are able to reproduce (i) the slope of colour-magnitude relation by Bower et al. (1992); (ii) the UV excess as measured by the colour (1550–V), (iii) the mass to blue luminosity ratio $(M/L_B)_{\odot}$ of elliptical galaxies. For all other details see Tantaló et al. (1997).

2.2. The gradients

In Fig. 1 we compare the theoretical and observational gradients in broad-band colors (left panel) and line strength indices (right panel). The radial distance is expressed in units of the effective radius and in *Kpc* respectively. The data are from Carollo & Danziger (1994a). Remarkably, while these models match the gradient in broad band colors which reflects the gradient in metallicity (cf. Table 1), they somewhat fail as far as the gradient in line strength indices Mg_2 and $\langle Fe \rangle$ are concerned. In brief, while the central value of Mg_2 and at some extent its gradient are matched (see the top left panel of Fig. 1), this is not the case of the $\langle Fe \rangle$ index (bottom left panel of Fig. 1). The theoretical gradients are $[\Delta \ln Mg_2 / \Delta R] \simeq -0.13$ and $[\Delta \ln \langle Fe \rangle / \Delta R] \simeq -0.11$ with R the galactocentric distance in *Kpc*. The gradients are nearly identical.

This is a surprising result because looking at the data of Table 1 the duration of star formation was much longer

Table 1. Basic features of the reference model.

parameter	1 st Shell	2 nd shell
$M_{L,12}$	0.146	0.150
ν	7.1	50.0
τ	0.74	0.29
$t_{g\omega}$	5.12	0.79
Z_{max}	0.0964	0.0439
$\langle Z \rangle$	0.0365	0.0286
$G(t)$	0.004	0.010
$S(t)$	0.845	0.874
N_{enh}	45.7%	53.9%

in the central core than in the outer shell (the same trend holds for all remaining shells not considered here), which implies that the stars in the core are on the average less α -enhanced than in the more external regions (cf. the temporal evolution of the elemental abundances shown in Fig. 2), whereas the gradients we have obtained seem to indicate a nearly constant ratio $[Mg/Fe]$.

In order to cast light on this contradiction we examined the variation of the abundance ratios $[Fe/H]$, $[C/Fe]$, $[O/Fe]$ and $[Mg/Fe]$ (with respect to the solar value) as a function of the metallicity and time, and the present-day number frequency distribution, $N(Z)$ (thereinafter the metallicity partition function), of living stars in different metallicity bins. The simultaneous inspection of the abundance ratios as a function of the metallicity (and hence age) and their partition function $N(Z)$ gives immediately an idea of the fraction of stars still existing in the stellar mix with metallicity above any particular value and with abundance ratios above or below the solar value. These relationships are shown in the two panels of Fig. 3 (the left panel is for the central core, 1st shell; the right panel is for the 2nd more external shell).

To further clarify the question we also look at the current age of the stellar population stored in every metallicity (we remind the reader that the metallicity in this model is a monotonic increasing function of the age, cf. Fig. 2). The top axis of Fig. 3 shows the correspondence between metallicity and birth-time of the stellar content of each metallicity bin, shortly named single stellar population (SSP). The SSP birth-time is $t = T_G - T_{SSP}$, where T_G is the present-day galaxy age and T_{SSP} is the current age of the SSP.

What we learn from this figure is that the external shell is truly richer in α -enhanced stars ($\sim 53.9\%$ of the total) than the inner one ($\sim 45.7\%$ of the total). These

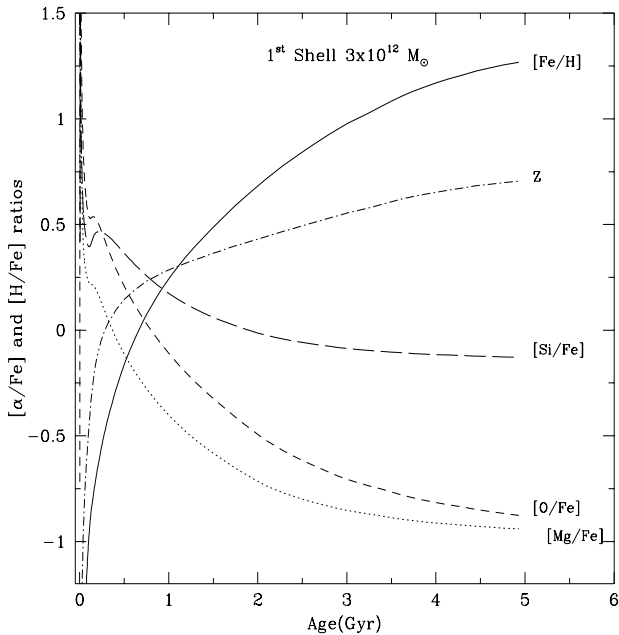


Fig. 2. Temporal evolution of four abundance ratios: $[\text{Fe}/\text{H}]$ (solid line), $[\text{Mg}/\text{Fe}]$ (dotted line), $[\text{O}/\text{Fe}]$ (dashed line), and $[\text{Si}/\text{Fe}]$ (long-dashed line). The dot-dashed line shows the ratio Z/Z_{\odot} as a function of time. The ratios are in the standard notation

percentages N_{enh} are given in Table 1. This confirms our expectation that these models should predict gradients in line strength indices consistent with the gradients in abundances.

Which is the reason for such unexpected contradiction?

One may argue that the above disagreement results either from the particular galactic model used to perform the comparison or the adoption of calibrations, such as those by Worthey (1992) and Worthey et al. (1994), which include the dependence on $[\text{Fe}/\text{H}]$, T_{eff} and gravity but neglect the effect of enhancing the α -elements. Therefore before proceeding further we have to check whether the usage of other calibrations for the line strength indices and/or galactic models would change the above conclusion.

3. Testing the sensitivity of Mg_2 to calibrations and chemistry

To answer the question posed in the previous section, first we change the calibration in usage adopting a new one in which the effects of $[\text{Mg}/\text{Fe}]$ are explicitly taken into account, and second we discuss different, *ad hoc* designed, galactic models in which different levels of enhancement in α -elements are let occur by artificially changing the history of star formation.

Table 2. Basic properties of test models. Model-A: late galactic wind and no enhancement of α -elements. Model-B: early galactic wind and enhancement of α -elements. Model-C: recent burst of star formation, and galactic wind, and strong enhancement of α -elements.

parameter	Model A	Model B	Model C
$M_{L,12}$	0.146	0.146	0.146
ν	7.1	100.0	$0.1 \div 50$
τ	0.74	0.05	0.10
$t_{g\omega}$	5.12	0.39	3.58
Z_{max}	0.0964	0.0713	0.0878
$\langle Z \rangle$	0.0365	0.0279	0.0294
$G(t)$	0.004	0.002	0.003
$S(t)$	0.845	0.942	0.994
N_{enh}	45.7%	85.2%	74.8%

3.1. Moving to calibrations containing $[\text{Mg}/\text{Fe}]$

Many studies have emphasized that line strength indices depend not only on the stellar parameters T_{eff} and gravity, but also on the chemical abundances (Barbuy 1994, Idiart et al. 1995, Weiss et al. 1995, Borges et al. 1995). The recent empirical calibration by Borges et al. (1995) include the effect of different $[\text{Mg}/\text{Fe}]$ ratios. The calibration is

$$\ln \text{Mg}_2 = -9.037 + 5.795 \cdot \frac{5040}{T_{\text{eff}}} + 0.398 \cdot \log g + 0.389 \left[\frac{\text{Fe}}{\text{H}} \right] - 0.16 \left[\frac{\text{Fe}}{\text{H}} \right]^2 + 0.981 \left[\frac{\text{Mg}}{\text{Fe}} \right] \quad (3)$$

which holds for effective temperatures and gravities in the ranges $3800\text{K} < T_{\text{eff}} < 6500\text{K}$ and $0.7 < \log g < 4.5$. From this equation we are able to analyse the effect of different $[\text{Mg}/\text{Fe}]$ enhancement.

Using equation (3) one has to adopt a different relation between the global metallicity Z and $[\text{Fe}/\text{H}]$ with respect to the standard one (cf. Bertelli et al. 1994). In fact, if the ratio $[\alpha/\text{Fe}]$ is enhanced with respect to the solar value, at given total metallicity the net $[\text{Fe}/\text{H}]$ must be scaled accordingly. We find that the general relation in presence of α -enhancement is

$$\left[\frac{\text{Fe}}{\text{H}} \right] = \log \left(\frac{Z}{Z_{\odot}} \right) - \log \left(\frac{X}{X_{\odot}} \right) - 0.8 \left[\frac{\alpha}{\text{Fe}} \right] - 0.05 \left[\frac{\alpha}{\text{Fe}} \right]^2 \quad (4)$$

The above relations for Mg_2 and $[\text{Fe}/\text{H}]$ are used to generate new SSPs and galactic models in which not only

the chemical abundances are enhanced with respect to the solar value but the effect of this on the line strength indices is taken into account in a self-consistent manner.

3.2. Three artificial galaxies

We present here three galactic models that in virtue of their particular history of star formation, have different chemical structures and degree of enhancement in α -element.

Model-A: late galactic wind. This case has late galactic wind (~ 5.12 Gyr), which means that the Type Ia dominate the enrichment in Fe of the gas, and the ratio $[\alpha/\text{Fe}]$ is solar or below solar for most of the time. This model is actually the central region of the $3 \times 10^{12} M_{\odot}$ galaxy presented above. The percentage (N_{enh}) of α -enhanced stars that are still alive at the age of 15 Gyr amounts to 45.7%.

Model-B: early galactic wind. In order to enhance the relative abundance of elements from Type II supernovae we arbitrarily shortened the duration of the star forming period. To this aim, in the central region of the same galaxy, the efficiency of star formation has been increased ($\nu = 100$) and the infall time scale decreases ($\tau = 0.05$ Gyr) so that the galactic wind occurs much earlier (at 0.39 Gyr) than in the previous case. The material (gas and stars) of Model-B is therefore strongly enhanced in α -elements. The percentages (N_{enh}) of α -enhanced stars that are still alive at the age of 15 Gyr amounts to 87.2%.

Model-C: recent burst of star formation. A third possibility is considered, in which a burst of star formation can occur within a galaxy that already underwent significant star formation and metal enrichment during its previous history. This model (always limited to the central region of the galaxy) has nearly constant star formation rate from the beginning, but at the age (arbitrarily chosen) of 3 Gyr it is supposed to undergo a sudden increase perhaps induced by a merger. Accordingly, the specific efficiency of star formation ν goes from $\nu = 0.1$ to $\nu = 50$ over a time scale of 10^8 yr. The initial nearly constant stellar activity is secured adopting a long time scale of gas accretion in the infall scheme ($\tau = 10$ Gyr). The rate of star formation as a function of time in units of $M_{\odot} \text{yr}^{-1}$ is given in Fig. 4. Soon after the intense period of star formation, the galactic wind occurs thus halting star formation and chemical enrichment. The basic chemical properties of the model as a function of the age are shown in Fig. 5. This displays the maximum (*dotted line*) and mean metallicity (*solid line*), and the fractionary mass of gas $G(t)$ (*dotted line*) and stars $S(t)$ (*solid line*) both normalized to the asymptotic galactic mass in units of $10^{12} M_{\odot}$. The percentage (N_{enh}) of α -enhanced stars that are still alive at the age of 15 Gyr amounts to 74.5%.

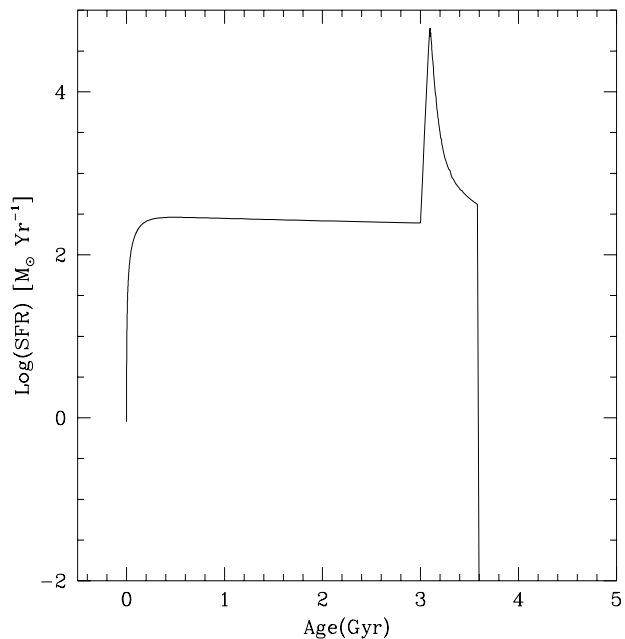


Fig. 4. *Model-C:* the star formation rate as a function of the time for the central region of the galaxy model with $3 \times 10^{12} M_{\odot}$. At the age of 3 Gyr the efficiency of the SFR is let increase from $\nu = 0.1$ up to $\nu = 50$ over a time scale of 10^8 yr. The parameters of this model are given in Table 2.

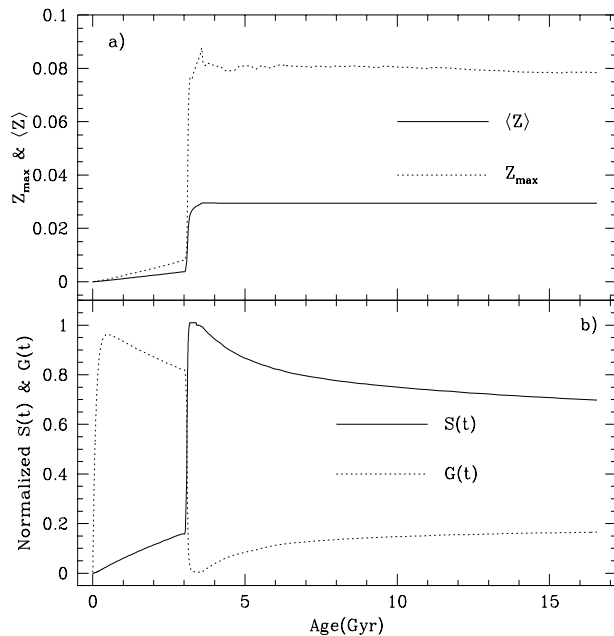


Fig. 5. *Model-C:* Panel (a) shows maximum and mean metallicity *dotted* and *solid line*, respectively. Panel (b) shows the fractionary density of gas $G(t)$ and living stars $S(t)$ as a function of time, *dotted* and *solid line*, respectively.

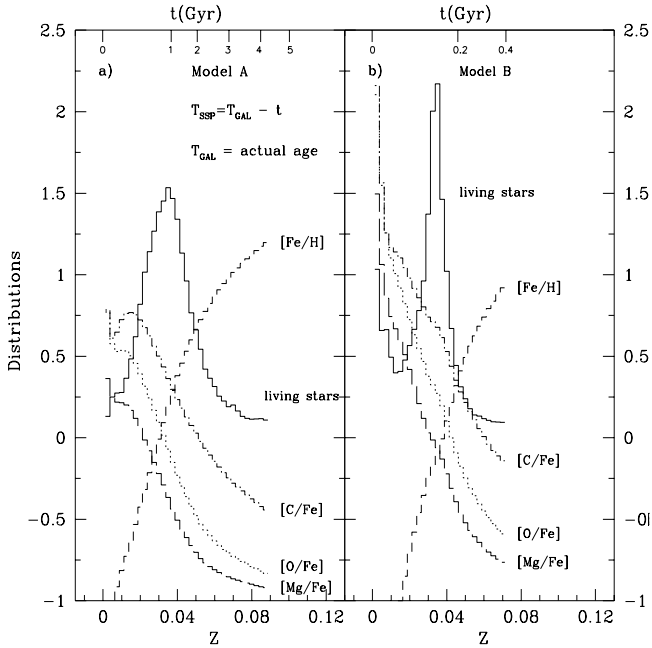


Fig. 6. The partition function $N(Z)$ and abundance ratios distribution per metallicity bin, for the Model-A (panel a) and Model-B (panel b). The *solid line* is $N(Z)$ in units of 10^{11} at the age of 15 Gyr. The *dotted*, *dashed*, *long-dashed*, and *dot-dashed* lines give the distribution per metallicity bin for $[O/Fe]$, $[Fe/H]$, $[Mg/Fe]$ and $[C/Fe]$, respectively. The abundance ratios are in the standard notation. The top scale gives the birth-time $t = T_G - T_{SSP}$ of a SSP with age T_{SSP} in a galaxy with age T_G .

3.3. The experiments

The basic data for the three models in question are summarized in Table 2, whereas their histories of chemical abundances together with the present-day partition function $N(Z)$ are shown in Figs. 6 (left panel for Model-A, right panel for Model-B) and 7 for Model-C. These figures are the analog of Fig. 3.

The distribution of chemical abundances (and their ratios) as a function of the total metallicity and/or time is used to calculate SSPs of different Z , $[Fe/H]$, $[O/Fe]$, $[Mg/Fe]$ for which with the aid of equations (3) and (4) we derive the corresponding Mg_2 index.

The procedure goes as follows: assigned the total metallicity Z we read from Figs. 6 or 7 the ratios $[C/Fe]$, $[O/Fe]$, and $[Mg/Fe]$. We derive $[Fe/H]$ from equation (4) and insert $[O/Fe]$ and $[Fe/H]$ into equation (3). It goes without saying that $[Fe/H]$ read derived from Figs. 6 or 7 and equation (4) are mutually consistent by definition.

Even if we will always refer to the ratio $[Mg/Fe]$, to quantify the level of enhancement in α -elements we prefer to adopt the ratio $[O/Fe]$, because our chemical models of galaxies somewhat underestimate the ratio $[Mg/Fe]$ as compared to the observational value. This is due to

the fact that the chemical models of galaxies by Portinari et al. (1997) over-estimate the production of Fe by the Type II supernovae (cf. Thielemann et al. 1993, 1996). This marginal drawback of the chemical model does not however affect the conclusion of this analysis.

The method to calculate the line strength index Mg_2 is the same as in Bressan et al. (1996) but for the different calibration.

Table 3 shows the values of $[Fe/H]$ and $[O/Fe]$ assigned to the SSPs according to chemical structure of Model-A, Model-B and Model-C, and for purposes of comparison to the reference SSPs with no enhancement at all.

The temporal evolution of Mg_2 index for the SSPs with different total metallicity and ratios $[O/Fe]$, and $[Fe/H]$ given in Table 3, is shown in the six panels of Fig. 8.

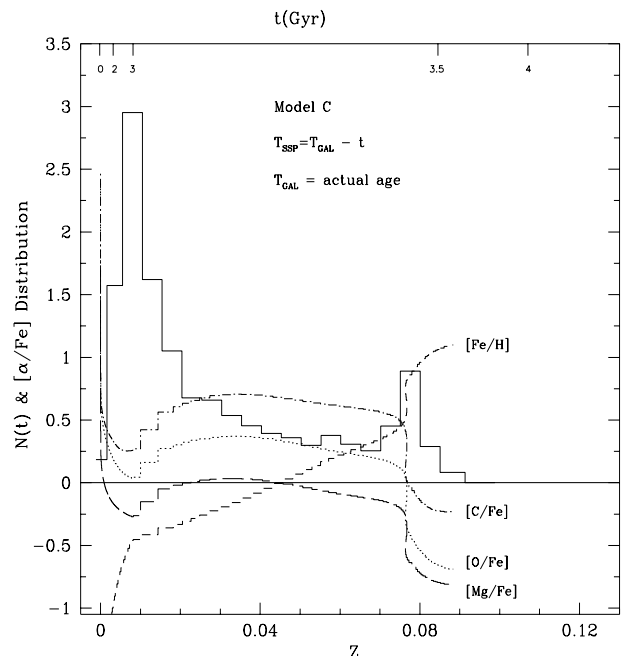


Fig. 7. The number of living stars and abundance ratios distribution per metallicity bin, for the Model-C. The abundance ratios are in the standard notation. The *solid line* is distribution of living stars in units of 10^{11} . The *dotted*, *dashed*, *long-dashed*, and *dot-dashed* lines give the distribution per metallicity bin for $[O/Fe]$, $[Fe/H]$, $[Mg/Fe]$ and $[C/Fe]$, respectively. The top scale gives the birth-time $t = T_G - T_{SSP}$ of a SSP with age T_{SSP} in a galaxy with age T_G .

The Mg_2 index of SSPs. It is soon evident that in absence of enhancement in α -elements (right panels of Fig. 8), Mg_2 monotonically increases with the metallicity, but for the extreme SSP with $Z=0.1$ for which the trend is reversed at ages older than 5 Gyr. When the enhancement of α -elements is included the trend Mg_2 -metallicity Z is reversed soon after Z get larger than solar (left panels of Fig. 8).

Table 3. [O/Fe] and [Fe/H] ratios for SSPs with enhancement of α -elements according to Model-A, Model-B and Model-C. The same ratios for the reference SSPs with no enhancement all are also shown.

Z	Model-A		Model-B		Model-C		Reference SSPs	
	[O/Fe]	[Fe/H]	[O/Fe]	[Fe/H]	[O/Fe]	[Fe/H]	[O/Fe]	[Fe/H]
0.0004	+0.8	-2.38	+3.28	-4.87	+0.51	-2.13	0.0	-1.71
0.004	+0.6	-1.22	+1.72	-2.23	+0.14	-0.82	0.0	-0.71
0.008	+0.5	-0.80	+1.22	-1.44	+0.03	-0.42	0.0	-0.39
0.02	+0.4	-0.30	+0.72	-0.57	+0.30	-0.22	0.0	+0.03
0.05	-0.50	+0.88	-0.25	+0.69	+0.31	+0.24	0.0	+0.50
0.1	-0.80	+1.55	-0.59	+1.40	-0.87	+1.60	0.0	+0.95

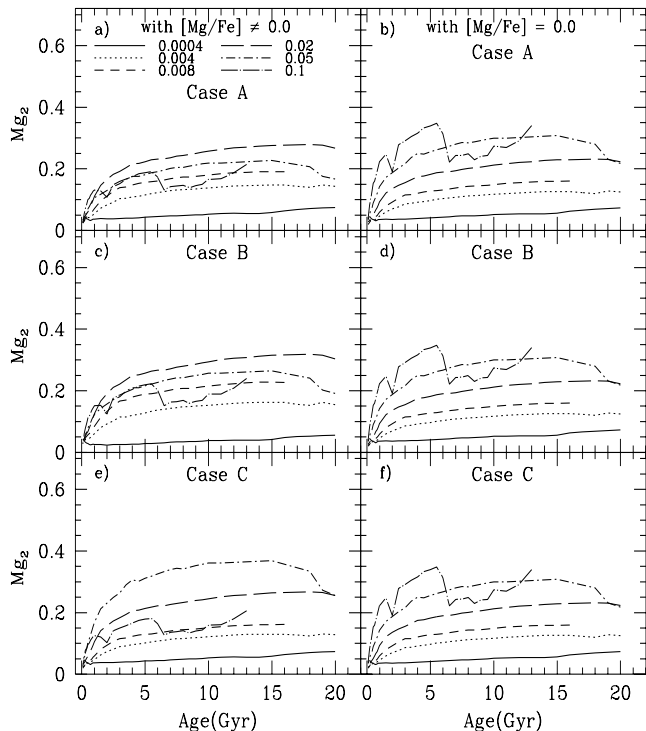


Fig. 8. Panels (a), (c) and (e) show the Mg_2 index evolution for SSPs with different metallicity (as indicated) and the assumption of enhancement in α -elements. Panels (b), (d) and (f) show the same but without enhancement of α -elements.

The Mg_2 index of galaxies. What the results for the Mg_2 index would be when applying these SSPs with the Borges et al. (1995) calibration to model galaxies? The situation is displayed in the various panels of Fig. 9 for Model-A and Model-B and in Fig. 10 for Model-A and C. The combined analysis of the chemical structures, partition functions $N(Z)$, and temporal variations of the Mg_2 index of the model galaxies (top panels of Figs. 9 and 10), the following remarks can be made

- (i) $[Mg/Fe] \neq 0$: Mg_2 in Model-A (late wind, no chemical enhancement) is always weaker than in Model-B (early wind, significant chemical enhancement). However, the difference is large for ages younger than about 5 Gyr, and gets very small up to vanishing for older ages. Mg_2 of Model-C is always weaker than Model-A and Model-B which means that the higher (or comparable) enhancement in α -elements of Model-C with respect to the previous ones does not produce a stronger Mg_2 index.
- (ii) $[Mg/Fe] = 0$: Mg_2 in Model-A (late wind, no chemical enhancement) is first weaker than in Model-B (early wind, significant chemical enhancement) up to ages of about 5 Gyr, and then becomes significantly stronger at older ages. Finally, the Mg_2 index of Model-C (burst of star formation, and strong enhancement) is weaker or about equal to that of Model-A and Model-B.

The intensity of the Mg_2 index does not simply correlate with the abundance of Mg and in particular with the ratio $[Mg/Fe]$. What causes this odd behaviour of the Mg_2 index as a function of the age and underlying chemical structure of the model galaxy?

To answer this question, we have artificially removed from the partition function $N(Z)$ all the stars in certain metallicity bins and recalculated the line strength indices for the three models.

Panels (c) and (d) of Figs. 9 and 10 show the results when all stars with metallicity higher than $Z=0.05$ are removed. This is motivated by the trend as function of the metallicity shown by the SSPs we have already pointed out. The situation remains unchanged.

Likewise, panels (e) and (f) of Figs. 9 and 10 show the same but when all stars with metallicity lower than $Z=0.008$ are removed. Now the results change significantly. In the case of $[Mg/Fe] \neq 0$, the Mg_2 index of Model-B is always much stronger than that of Model-A. In such a case there is correspondence between the strength of the index and the amount of enhancement in α -elements. In contrast for $[Mg/Fe] = 0$, at younger ages Mg_2 of Model-B is stronger at younger ages, but equals

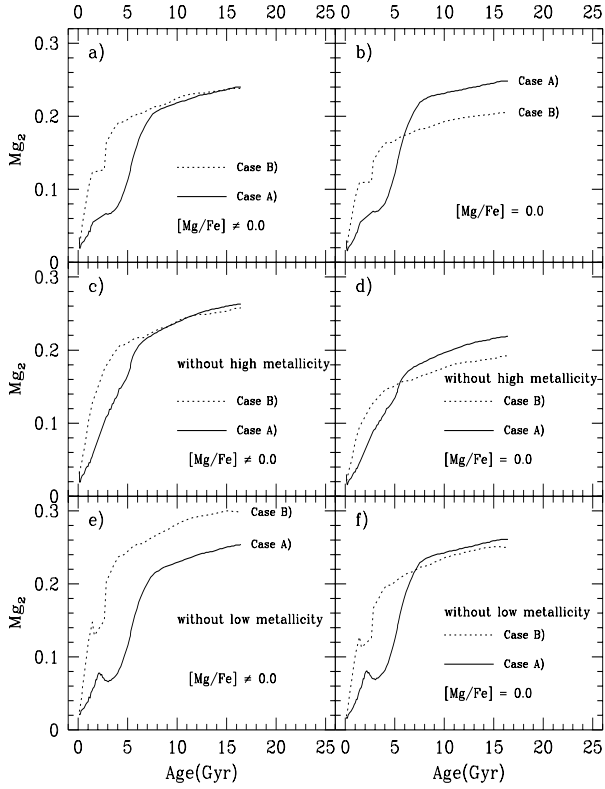


Fig. 9. Evolution of the Mg_2 index as a function of time. *Panels (a), (c) and (e)* show the evolution of the Mg_2 index calculated including the effect of the chemical abundances, while *Panels (b), (d) and (f)* show the same but without the effect of α -enhancement. The *solid line* corresponds to Model-A and the *dotted line* to Model-B.

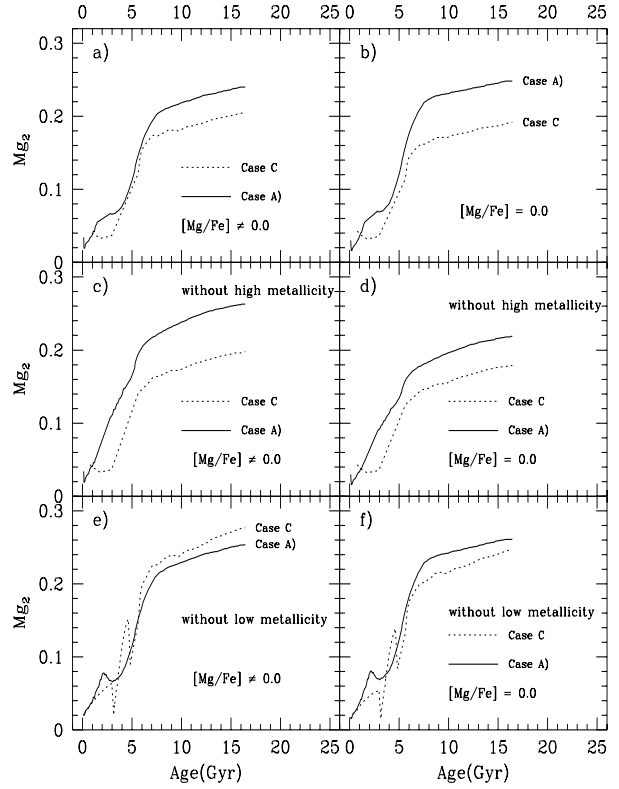


Fig. 10. Evolution of the Mg_2 index as a function of time. *Panels (a), (c) and (e)* show the evolution of the Mg_2 index calculated including the effect of the chemical abundances, while *Panels (b), (d) and (f)* show the same but without the effect of α -enhancement. The *solid line* corresponds to Model-A and the *dotted line* to Model-C.

(or even get weaker) that of Model-A at older ages. The same can be said comparing Model-A to Model-C.

What we learn from these experiments is that

- *the index Mg_2 heavily depends on the underlying partition function $N(Z)$, which of course is not known, so that inferring either the abundance of Mg or the enhancement ratio $[Mg/Fe]$ is a cumbersome affair.*
- *The observational gradients in Mg_2 (and $\langle Fe \rangle$) do not automatically imply gradients in chemical abundances or enhancement ratios.*

4. Gradients across galaxies: a basic tool

What do we learn from the gradients in line strength indices across galaxies?

Analyzing the gradients in H_β and $[Mg/Fe]$ measured in the Gonzales (1993) sample of elliptical galaxies, Bressan et al. (1996) translated those gradients into age and metallicity gradients and grouped the galaxies of the sample in four sub-classes according to whether the nucleus turned out to be older or younger and more or less metal-rich than the external regions. The majority of galaxies

fell into the group with the nucleus containing a fraction of stars younger and more metal-rich than the external regions. In this section we intend to check whether or not the gradients in age and metallicity suggested by Bressan et al. (1996) are consistent with the gradients Mg_2 and $\langle Fe \rangle$ discussed in this paper.

To this purpose we calculate the partial derivatives ∂Mg_2 , $\partial \langle Fe \rangle$ and ∂H_β with respect to metallicity, age, and $[Mg/Fe]$ of SSPs

$$\frac{\partial Mg_2}{\partial \log Z/Z_\odot} \Big|_{t, [Mg/Fe]} \quad \frac{\partial Mg_2}{\partial [Mg/Fe]} \Big|_{t, Z} \quad \frac{\partial Mg_2}{\partial \log t} \Big|_{Z, [Mg/Fe]}$$

$$\frac{\partial \langle Fe \rangle}{\partial \log Z/Z_\odot} \Big|_{t, [Mg/Fe]} \quad \frac{\partial \langle Fe \rangle}{\partial [Mg/Fe]} \Big|_{t, Z} \quad \frac{\partial \langle Fe \rangle}{\partial \log t} \Big|_{Z, [Mg/Fe]}$$

$$\frac{\partial H_\beta}{\partial \log Z/Z_\odot} \Big|_{t, [Mg/Fe]} \quad \frac{\partial H_\beta}{\partial [Mg/Fe]} \Big|_{t, Z} \quad \frac{\partial H_\beta}{\partial \log t} \Big|_{Z, [Mg/Fe]}$$

The indices Mg_2 , $\langle Fe \rangle$, and H_β of the SSP are obtained as follows: given the total metallicity Z and enhancement ratio $[Mg/Fe]$, we derive from eq. (4) the corresponding

value of $[Fe/H]$ to be used in the calibration of Borges et al. (1995) for Mg_2 (eq. 3) and Worthey (1992) and Worthey et al. (1994) for $\langle Fe \rangle$ (F_{e5335} and F_{e5270}) and H_β . A summary of the Mg_2 , $\langle Fe \rangle$ and H_β indices of SSP with different Z and age is given in Table 4.

With the aid of these SSP we express the mean variation δMg_2 , $\delta \langle Fe \rangle$ and δH_β as a function of $[Mg/Fe]$, Z , and t :

$$\delta Mg_2 = 0.1056 \times \Delta \left[\frac{Mg}{Fe} \right] + 0.1765 \times \Delta \log \left(\frac{Z}{Z_\odot} \right) + 0.0890 \times \Delta \log t \quad (5)$$

$$\delta \langle Fe \rangle = -0.9606 \times \Delta \left[\frac{Mg}{Fe} \right] + 1.8928 \times \Delta \log \left(\frac{Z}{Z_\odot} \right) + 0.7021 \times \Delta \log t \quad (6)$$

$$\delta H_\beta = -2079 \times \Delta \left[\frac{Mg}{Fe} \right] - 0.3796 \times \Delta \log \left(\frac{Z}{Z_\odot} \right) - 1.2072 \times \Delta \log t \quad (7)$$

Table 4. New SSPs with different metallicity and $[Mg/Fe]$.

Age(Gyr)	Z	[Mg/Fe]	[Fe/H]	Mg_2	$\langle Fe \rangle$	H_β
15	0.004	+0.3	-0.952	0.134	1.714	1.687
15	0.004	0.0	-0.707	0.125	1.931	1.710
15	0.004	-0.3	-0.472	0.115	2.165	1.750
15	0.02	+0.3	-0.214	0.262	2.787	1.312
15	0.02	0.0	+0.031	0.229	3.087	1.377
15	0.02	-0.3	+0.266	0.198	3.395	1.452
15	0.05	+0.3	+0.253	0.365	3.606	1.197
15	0.05	0.0	+0.497	0.308	3.937	1.279
15	0.05	-0.3	+0.733	0.258	4.276	1.368
5	0.004	+0.3	-0.952	0.104	1.401	2.388
5	0.004	0.0	-0.707	0.097	1.630	2.415
5	0.004	-0.3	-0.472	0.090	1.875	2.455
5	0.02	+0.3	-0.214	0.211	2.431	1.884
5	0.02	0.0	+0.031	0.182	2.734	1.945
5	0.02	-0.3	+0.266	0.155	3.050	2.018
5	0.05	+0.3	+0.253	0.308	3.235	1.648
5	0.05	0.0	+0.497	0.255	3.584	1.734
5	0.05	-0.3	+0.733	0.210	3.943	1.828

To evaluate and visually show the size of $\delta \langle Fe \rangle$ and δMg_2 at varying $[Mg/Fe]$, Z , and t , we calculate the *age*, *metallicity*, and *enhancement vectors* shown in Fig. 11 for fixed variations of age, metallicity, and $[Mg/Fe]$: the age goes from 5 to 15 Gyr, the metallicity from 0.004 to 0.05,

and the $[Mg/Fe]$ ratio from -0.3 to 0.4 dex (the length of the vectors is $\Delta \log(Z) \sim 1.1$, $\Delta[Mg/Fe] \sim 0.7$ and $\Delta \log(t) \sim 0.47$). The vectors are centered on $(0,0)$, i.e. null variation.

There are two important points to remark:

- The well known age-metallicity degeneracy given that the age and metallicity vectors run very close each other.
- The enhancement vector is almost orthogonal to the other two, which allows us to separate its effects from the combined ones of age and metallicity.

In the same diagram we show data for three galaxies, namely NGC 2434, NGC 6407 and NGC 7192 taken from Carollo & Danziger (1994a). The displayed data are the difference between the local value of each index (at any radial distance) and its value at the center. Taking the galaxy NGC 7192 as a prototype, we first derive an eye estimate of the mean slope of the data, second we translate the origin of the vectors to some arbitrary external point of the galaxy. The result is that with respect to its external regions, the nucleus is either more metal-rich and older or more metal-rich and slightly younger, and in any case more enhanced in $[Mg/Fe]$. It goes without saying that if the nucleus is older than the periphery a lower increase in the metallicity toward the center is required than in the opposite alternative (younger nucleus). In such a case the increase in metallicity must be large enough to compensate for the opposite trend of the age. Similar considerations apply also to the galaxies NGC 2434 and NGC 6407.

How this result conforms with the Bressan et al. (1996) analysis of Gonzales (1993) galaxies in the H_β and $[Mg/Fe]$, suggesting that in most galaxies the nucleus was younger (star formation lasted longer) and more metal-rich than the external regions?

Table 5. Estimated gradients in age, metallicity and α -enhancement across two galaxies of the Carollo & Danziger (1994a) sample. The nuclear region is the one inside 5 arcsec from the centre. Ages are in Gyr.

NGC	Mg_{2N}	$\langle Fe \rangle_N$	$H_{\beta N}$	Mg_{2E}	$\langle Fe \rangle_E$	$H_{\beta E}$
2434	0.235	2.65	2.2	0.194	2.42	1.8
3706	0.288	2.96	1.8	0.229	2.52	1.8
NGC	δMg_2	$\delta \langle Fe \rangle$	δH_β	$\Delta \left[\frac{Mg}{Fe} \right]$	$\Delta \log \left(\frac{Z}{Z_\odot} \right)$	$\Delta \log(t)$
2434	-0.041	-0.225	-0.400	-0.159	-0.377	0.4776
3706	-0.059	-0.440	0.000	-0.106	-0.332	0.1229

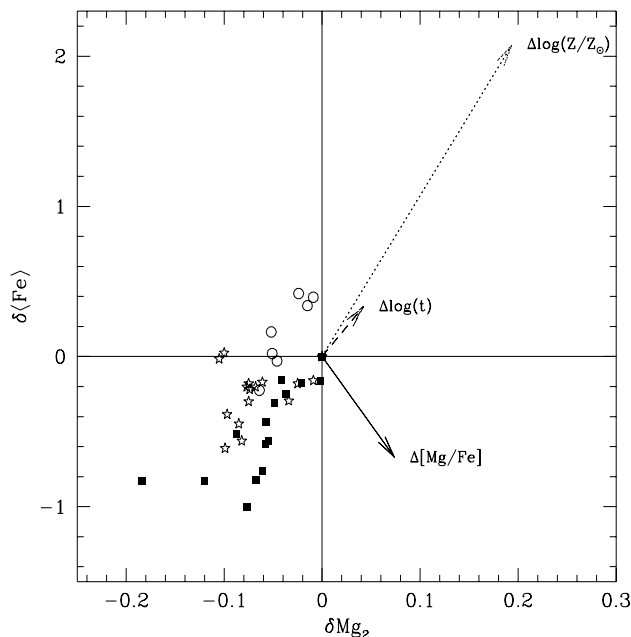


Fig. 11. The $\delta\langle\text{Fe}\rangle$ versus δMg_2 relation. The three arrows centered on (0,0) indicate the *age*, *metallicity*, and *enhancement* vectors as indicated. Along the age vector, the age goes from 5 to 15 Gyr, along the metallicity vector Z ranges from 0.004 to 0.05, and along the enhancement vector $[\text{Mg}/\text{Fe}]$ goes from -0.3 to 0.4 dex. The data are from Carollo & Danziger (1994a) for NGC 2434, NGC 6407 and NGC 7192, *open circles*, *open stars*, and *filled squares*, respectively.

To answer the above question we make use of the H_β index, known to be more sensitive to the age, and look at the parameter space H_β , Mg_2 and $\langle\text{Fe}\rangle$. Unfortunately, to our knowledge this type of analysis is feasible only for two galaxies of the Carollo & Danziger (1994a,b) catalog for which all the data are available. These are summarized in Table 5. The top part of the table shows the observational data, i.e. the mean values of Mg_2 , $\langle\text{Fe}\rangle$, and H_β of the central region (indicated by a capitol N) and the external region (labelled by a capitol E). The two regions are defined by the visual inspection of the gradients in Mg_2 and the transition distance is seen to occur at 5 arcsec from the galactic centre (cf. Carollo & Danziger 1994a). The bottom part of Table 5 lists the difference δMg_2 , $\delta\langle\text{Fe}\rangle$, and δH_β between the external and central values of the three indices, and the solution found solving the system of equations (5), (6) and (7). The solution consists in the differences $\Delta[\text{Mg}/\text{Fe}]$, $\Delta\log(Z/Z_\odot)$, and $\Delta\log(t)$ between the periphery and centre. It turns out that both galaxies have the nuclear region containing stars more enhanced in α -elements, more metal-rich, and younger than the external regions.

5. Going from galaxy to galaxy

Given that central values of H_β , Mg_2 , and $\langle\text{Fe}\rangle$ are known to vary from galaxy to galaxy, what the implications are as far as the differences in age, metallicity, and enhancement in α -elements are concerned?

To answer this question we make use of a small sample of galaxies (29 objects in total) selected by Worthey (1992) from the Gonzales (1993) catalog. These galaxies are thought to possess the best determined line strength indices. The data are presented in Table 6. Column (1) identifies the galaxy: those objects whose name is followed by a V belong to the Virgo cluster. Columns (2) to (6) give H_β , $[\text{Mg}/\text{Fe}]$, Mg_2 , Fe_{5270} and Fe_{5335} and velocity dispersion σ_0 (Km sec^{-1}) for the Re/8 data (nucleus) of the Gonzales (1993) galaxies. Columns (7), (8) and (9) show the differences δH_β , δMg_2 , and $\delta\langle\text{Fe}\rangle$ of the galaxy indices with respect to the mean values (see below), respectively. Columns (10), (11), and (12) give the difference with respect to the mean of the enrichment factor $\Delta[\text{Mg}/\text{Fe}]$, metallicity $\Delta\log(Z/Z_\odot)$, and age $\Delta\log(t)$ found for each galaxy. Finally, column (13) lists the total absolute visual magnitude M_V .

For each set of data, we have calculated the mean values of Mg_2 , $\langle\text{Fe}\rangle$ and H_β to be used as the origin of a new system of coordinates in which the differences δMg_2 , $\delta\langle\text{Fe}\rangle$ and δH_β passing from galaxy to galaxy are plotted and compared to the age, metallicity, and enhancement vectors. The mean values are $\overline{H_\beta} = 1.72$, $\overline{\text{Mg}_2} = 0.31$, and $\overline{\langle\text{Fe}\rangle} = 3.12$.

5.1. The δMg_2 - $\delta\langle\text{Fe}\rangle$ and δMg_2 - δH_β planes

The observational data for the differences δMg_2 and $\delta\langle\text{Fe}\rangle$ are shown in Fig. 12, in which we have drawn the metallicity, enhancement, and age vectors, whose length is the same as in the previous analysis, and finally indicated the positions of M32 and NGC 4649, the prototype galaxies in the discussion below. The thick dashed line is the linear regression of the data.

Once again, age and metallicity cannot be safely separated, whereas this is feasible for $[\text{Mg}/\text{Fe}]$.

In order to cope with the age-metallicity degeneracy encountered in the δMg_2 - $\delta\langle\text{Fe}\rangle$ plane, we look at the δMg_2 - δH_β plane because H_β is known to be more sensitive to the age of the underlying stellar populations. This is shown in Fig. 13 where the moduli of the three vectors are: $\Delta\log(Z) \sim 1.1$, $\Delta[\text{Mg}/\text{Fe}] \sim 0.7$ and $\Delta\log(t) \sim 0.47$. In this figure the effect of $[\text{Mg}/\text{Fe}]$ and metallicity can not be isolated because the two vectors are coincident (degeneracy).

With the aid of the equations (5) (6) and (7) and the differences δH_β , δMg_2 , and $\delta\langle\text{Fe}\rangle$, we derive for each galaxy the variations in age $\Delta\log(t)$, metallicity $\Delta\log(Z/Z_\odot)$, and enhancement $\Delta[\text{Mg}/\text{Fe}]$ with respect to

Table 6. Basic data for galaxies of the Gonzales (1993) sample. The mean values of H_β , Mg_2 and $\langle Fe \rangle$ are $\overline{H_\beta} = 1.72$, $\overline{Mg_2} = 0.31$, and $\overline{\langle Fe \rangle} = 3.12$.

NGC	H_β	[MgFe]	Mg_2	Fe52	Fe53	σ_0	δMg_2	δH_β	$\delta \langle Fe \rangle$	$\Delta[\frac{Mg}{Fe}]$	$\Delta \log(\frac{Z}{Z_\odot})$	$\Delta \log(t)$	M_V
221	2.31	2.85	0.227	3.02	2.70	1.86	-0.0884	0.5938	-0.2603	-0.2801	-0.1303	-0.4027	-16.64
224	1.67	3.87	0.345	3.34	3.19	2.19	0.0296	-0.0462	0.1447	0.0844	0.1250	-0.0156	
315	1.74	3.74	0.323	3.08	3.14	2.51	0.0076	0.0238	-0.0103	0.0485	0.0334	-0.0386	-24.61
547	1.58	3.76	0.328	3.19	3.50	2.37	0.0126	-0.1362	0.2197	-0.0533	0.0496	0.1064	
584	2.08	3.54	0.295	3.21	2.96	2.29	-0.0204	0.3638	-0.0353	-0.0496	0.0733	-0.3159	-22.66
636	1.89	3.57	0.285	3.32	3.04	2.20	-0.0304	0.1738	0.0596	-0.1711	-0.0145	-0.1099	-21.57
821	1.66	3.65	0.333	3.29	3.03	2.28	0.0176	-0.0562	0.0396	0.0688	0.0487	0.0194	-22.59
1700	2.11	3.53	0.296	3.31	3.06	2.36	-0.0194	0.3938	0.0646	-0.0884	0.1185	-0.3483	-23.20
2300	1.68	3.84	0.352	3.27	3.04	2.40	0.0366	-0.0362	0.0346	0.1756	0.1217	-0.0385	-22.60
3377	2.09	3.23	0.283	2.91	2.66	2.03	-0.0324	0.3738	-0.3353	0.0302	-0.0510	-0.2988	-20.39
3379	1.62	3.69	0.324	3.22	3.00	2.31	0.0086	-0.0962	-0.0103	0.0396	-0.0140	0.0773	-21.13
4374 V	1.51	3.67	0.317	3.18	2.98	2.45	0.0016	-0.2062	-0.0403	0.0033	-0.0937	0.1997	-22.73
4478 V	1.84	3.56	0.243	4.04	2.89	2.11	-0.0724	0.1238	-0.1553	-0.2999	-0.2438	0.0258	-20.33
4552 V	1.47	3.92	0.355	3.22	3.28	2.40	0.0396	-0.2462	0.1297	0.1215	0.0705	0.1608	-21.68
4649	1.40	4.01	0.370	3.31	3.48	2.49	0.0546	-0.3162	0.2747	0.1246	0.1349	0.1981	-22.82
4697 V	1.75	3.36	0.300	3.31	3.05	2.21	-0.0154	0.0338	0.0597	-0.1071	-0.0219	-0.0027	-22.46
5638	1.65	3.63	0.325	3.17	2.85	2.19	0.0096	-0.0662	-0.1103	0.0962	-0.0268	0.0467	
5812	1.70	3.83	0.320	3.25	3.28	2.30	0.0046	-0.0162	0.1447	-0.0463	0.0510	0.0054	
5813	1.42	3.53	0.311	3.08	2.83	2.31	-0.0044	-0.2962	-0.1653	0.0200	-0.1889	0.3013	
5831	2.00	3.66	0.302	3.37	3.16	2.20	-0.0134	0.2838	0.1447	-0.1073	0.1158	-0.2530	-21.85
5846	1.45	3.76	0.340	3.18	2.99	2.35	0.0246	-0.2662	-0.0353	0.1173	-0.0379	0.2122	-22.84
6127	1.50	3.76	0.329	3.07	3.03	2.38	0.0136	-0.2162	-0.0703	0.0809	-0.0650	0.1856	
6703	1.88	3.55	0.304	3.23	3.01	2.26	-0.0114	0.1638	-0.0003	-0.0417	0.0298	-0.1379	
7052	1.48	3.77	0.338	3.18	3.18	2.44	0.0226	-0.2362	0.0596	0.0648	-0.0045	0.1859	
7454	2.15	2.84	0.236	2.72	2.44	2.03	-0.0794	0.4338	-0.5403	-0.1172	-0.2481	-0.2611	
7562	1.69	3.61	0.306	3.25	2.95	2.39	-0.0094	-0.0262	-0.0203	-0.0439	-0.0497	0.0449	
7619	1.36	3.93	0.370	3.36	3.48	2.48	0.0546	-0.3562	0.2997	0.1079	0.1252	0.2371	-23.36
7626	1.46	3.78	0.366	3.15	3.27	2.40	0.0506	-0.2562	0.0896	0.1984	0.0929	0.1489	-23.36
7785	1.63	3.66	0.324	3.14	3.15	2.38	0.0086	-0.0862	0.0246	0.0241	0.0004	0.0671	

the mean values. The results are listed in columns (10), (11) and (12) of Table 6.

Looking at M32 and NGC 4649 as an example, we get the following results: for M32 $\Delta \log(t) = -0.403$, $\Delta \log(Z/Z_\odot) = -0.130$, and $\Delta[Mg/Fe] = -0.280$; for NGC 4649 $\Delta \log(t) = 0.198$, $\Delta \log(Z/Z_\odot) = 0.135$, and $\Delta[Mg/Fe] = 0.124$. The stellar content of M32 is less metal rich, less enhanced in α -elements, and much younger (or more safely has a much younger component contributing to H_β) than NGC 4649.

5.2. The $\Delta \log(t)$, $\Delta \log(Z/Z_\odot)$, $\Delta[Mg/Fe]$ space

Aim of this section is to investigate whether systematic correlations exist among the three physical quantities $\Delta \log(t)$, $\Delta \log(Z/Z_\odot)$, and $\Delta[Mg/Fe]$. The occurrence of such relations would bear very much on the past history of star formation and chemical enrichment, and the mechanism of galaxy formation as well.

Before starting this part of the analysis it is worth clarifying the real meaning of the *age* parameter $\Delta \log(t)$. This age (being mainly controlled by H_β) actually refers to the younger components of the stellar mix in the galaxy (nucleus). In the ideal case (however possible) of continuous star formation from the early epochs it would mea-

sure the overall duration of the star forming activity. In the case that recurrent episodes have taken place (such as in mergers and/or bursts), it would measure the age of the last episode. Given these premises, we examine the following relationships:

Age-Z. The relation between $\Delta \log(Z/Z_\odot)$ and $\Delta \log(t)$ is shown in Fig. 14, where only a large scatter is seen (no systematic trend). The degree of metal enrichment seems to be totally unrelated to the age, in the sense that at any given metallicity all ages are possible. Does it mean that sporadic episodes of star formation may change the age parameter without significantly affecting the metallicity? It is worth recalling that H_β is very sensitive to recent star formation, and that a burst of stellar activity implying even a very small fraction of the galaxy mass would immediately increase H_β without affecting the metallicity (cf. Bressan et al. 1996). Furthermore, the recovery time of H_β after a burst is of order of about 1 Gyr, after which no trace of the star forming period would be easily detectable with the H_β diagnostic.

Age-[Mg/Fe]. The relationship between $\Delta[Mg/Fe]$ and $\Delta \log(t)$ is shown in Fig. 15. Now a good relation is found: older galaxies seem to be more enhanced in α -elements.

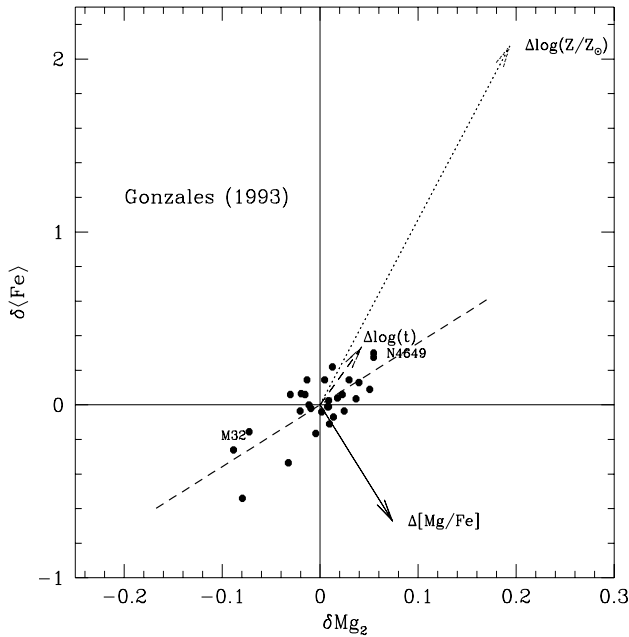


Fig. 12. The $\delta\langle\text{Fe}\rangle$ versus δMg_2 relation. The three arrows centered on (0,0) are the *age*, *metallicity*, and *enhancement vectors* as indicated. They have been calculated as in Fig.11. The displayed data are for each galaxy the difference between its central value and the mean value of the sample. The position of M32 and NGC 4649 are indicated. The *thick dashed line* is the linear regression of the data.

Z - $[\text{Mg}/\text{Fe}]$. The relationship between $\Delta[\text{Mg}/\text{Fe}]$ and $\Delta\log(Z/Z_\odot)$ is shown in Fig. 16. It appears that more metal-rich galaxies are also more enhanced in α -elements.

In order to cast light on the physical implications of the above relations, we correlate each of three quantities $\Delta\log(t)$, $\Delta\log(Z/Z_\odot)$, and $\Delta[\text{Mg}/\text{Fe}]$ to the total luminosity of the galaxy as measured by the absolute magnitude M_V . The discussion below would not change using M_B . The three relations are shown in Fig. 17 (age), 18 (metallicity), and 19 ($[\text{Mg}/\text{Fe}]$).

Age- M_V . Inspecting the distribution of galaxies in Fig. 17 we notice that in spite of the large scatter an important trend can be seen. First in our sample all galaxies but M32 are brighter than $M_V = -20$, which is the range of the classical color-magnitude relation of Bower et al. (1992). Second among the galaxies defining the upper edge of the distribution in age three of them, namely NGC 4374, NGC 4478, and NGC 4552, belong to the Virgo cluster, and according to Sweitzer & Seitzer (1992) they have either no sign or some evidence of mild interaction or rejuvenation. In the same region there are four more objects: NGC 3379 and NGC 7619 which have no sign of interaction (Sweitzer & Seitzer 1992), and NGC 4649 and NGC 5846, for which no special informa-

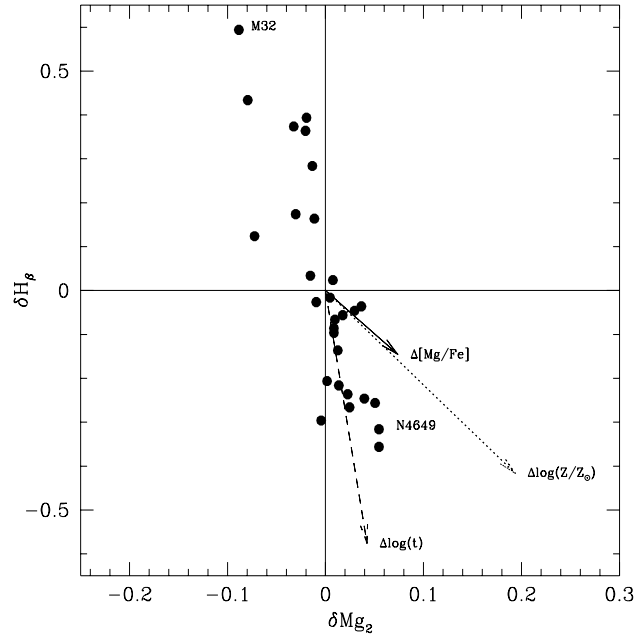


Fig. 13. The δH_β versus δMg_2 relation. The three arrows centered on (0,0) are the *age*, *metallicity* and *enhancement vectors* as indicated. They have been calculated as in Fig.11. The data are from Gonzales (1993) and for each galaxy the difference between its central values and the mean value of the sample are displayed. The positions of M32 and NGC 4649 are indicated.

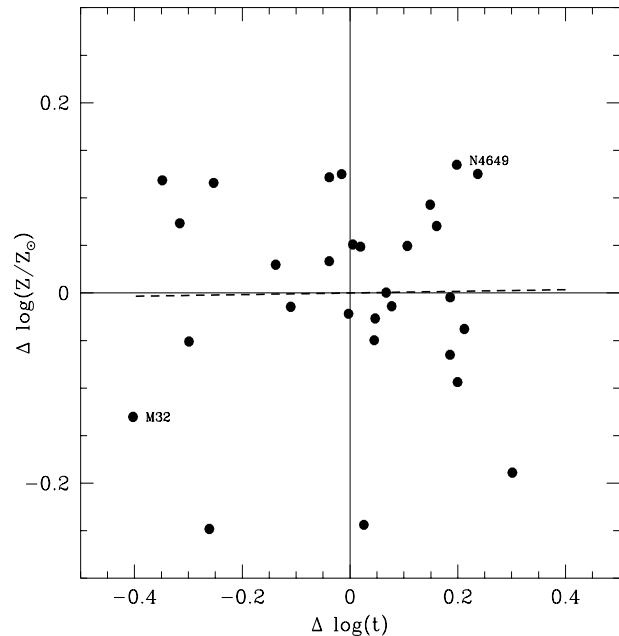


Fig. 14. The $\Delta\log(Z/Z_\odot)$ versus $\Delta\log(t)$ relation. The *thick dashed line* is the linear regression of the results. The position of M32 and NGC 4649 are indicated.

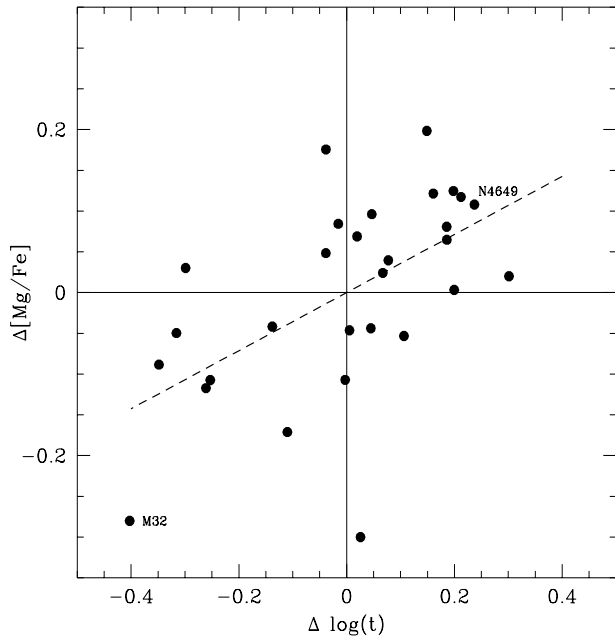


Fig. 15. The $\Delta[\text{Mg}/\text{Fe}]$ versus $\Delta \log(t)$ relation. The *thick dashed line* is the linear regression of the results. The position of M32 and NGC 4649 are indicated.

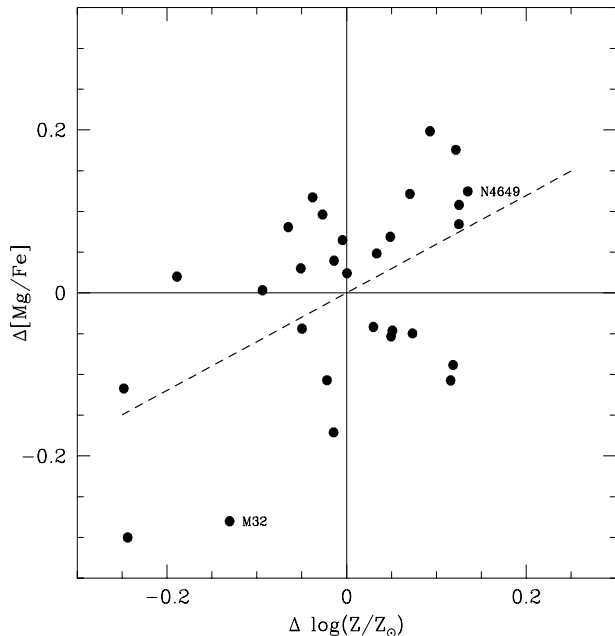


Fig. 16. The $\Delta[\text{Mg}/\text{Fe}]$ versus $\Delta \log(Z/Z_{\odot})$ relation. The *thick dashed line* is the linear regression of the results. The position of M32 and NGC 4649 are indicated.

tion is available. Finally, the last Virgo galaxy in our sample, namely NGC 4697, deviates from the relation defined by its companions in spite of its similar M_V and no signs of interaction (Sweitzer and Seitzer 1992). But for this latter case, all the above galaxies seem to cluster on a fairly tight relationship in which the last episode of star formation occurred earlier and earlier at increasing luminosity (likely mass of the galaxy). Is this the locus of non-interacting galaxies, along which we see the pristine star formation? If so, recalling the meaning of the age parameter in usage here this implies that star formation either started later or continued longer at decreasing galaxy mass (cf. Bressan et al. 1996 for a similar suggestion).

All other galaxies are much scattered along the age axis. Indeed most of them have sign of interaction or rejuvenation (Sweitzer & Seitzer 1992). Does it imply that more recent star formation has occurred altering H_{β} and age assignment in turn ?

M32 is an ambiguous case because either it could represent the continuation of the trend shown by the old galaxies, in which star formation lasted till a recent past or it has been rejuvenated by a recent episode. As compared to NGC 4649 there is factor 4.0 in between. Assuming the canonical age of 15 Gyr for the oldest galaxies, M32 terminated its star formation history or suffered from star formation about 3.75 Gyr ago.

In both cases the relatively young age of at least part of its stellar content is also indicated by studies of the classical color-magnitude diagram of the resolved stars (cf. Grillmair et al. 1996 and references therein). Grillmair et al. (1996) find that the CMD of M32 is consistent with a luminosity weighted age of about 8.5 Gyr and $[\text{Fe}/\text{H}]=-0.25$. There is however a significant component with $[\text{Fe}/\text{H}]=0$ for which younger ages cannot be excluded. Indeed an age of about 6 Gyr was suggested by O’Connell (1988 and references), of 5 Gyr by Freedman (1989), $4 \div 5$ Gyr by Freedman (1992). See also Elston & Silva (1992), Davidge & Jones (1992), and Hardy et al. (1994). Bressan et al. (1994) addressed the question of the M32 age using the spectral synthesis technique and reached the important conclusions: the bulk of stars have ages as old as those typical of globular clusters say in the range $13 \div 15$ Gyr, consistently with Grillmair’s et al. (1996) estimate; there is a younger component which cannot be older than 5 Gyr and younger than 1 Gyr. This latter boundary is set by the UV properties of M32 which has $(1550-V)=4.5$ (Burstein et al. 1988). See Bressan et al. (1994) for all other details.

$Z-M_V$. The relationship between $\Delta \log(Z/Z_{\odot})$ and M_V is shown in Fig. 18: the metallicity seems to increase with the luminosity (mass) of the galaxy. Limiting the inspection to the group of galaxies that where used to argue about the old age limit in Fig. 17, namely NGC 3379, NGC 4374, NGC 4478, NGC 4552, NGC 4649, NGC 5846, and NGC 7619, they seem to clus-

ter on the mean value but for NGC 4478, which is even more metal-poor than M32. In any case, also for this subset of galaxies the above trend is present. Remarkable is the case of all galaxies brighter than $M_V = -20$ and apparently younger than the mean age (cf. Fig. 17) whose metallicity is in contrast significantly above the mean value. Does this suggests that galaxies suffering from subsequent episodes of star formation further increase their metallicity? Finally, noticeable is the case of NGC 315, the brightest galaxy in the sample, which has age and metallicity only slightly below and above the mean, respectively. This somewhat weakens the notion that bright galaxies are also metal rich.

$[Mg/Fe]-M_V$. Fig. 19 shows the relation between $\Delta[Mg/Fe]$ and M_V . We start noticing that with the exception of NGC 4478, all other galaxies of the group defining the old age limit in Fig. 17 are enhanced in α -elements, whereas the remaining galaxies have a different degree of enhancement. It appears that not necessarily galaxies with high metallicity are also enhanced in α -elements, even if from the results shown in Fig. 16 some trend of this kind holds on a very broad sense. This can be explained recalling that star formation over periods of time longer than about 1 Gyr easily wipes out the signature type II supernovae in the abundance ratio $[\alpha/Fe]$ (cf. our model galaxies discussed in section 2).

6. Age ranking

Having established the relative differences $\Delta \log(t)$, $\Delta \log(Z)$, and $\Delta[Mg/Fe]$ from galaxy to galaxy, the absolute ranking of the central regions of different galaxies can be attempted. The zero point of the ranking scale is M32 for which we have independent estimates of the age, metallicity, and perhaps $[Mg/Fe]$. We adopt the age of $3.5 \div 4$ Gyr, $[Fe/H]=-0.25$, and $[Mg/Fe]=0$. The assignment of absolute ages is made with the aid of grids of SSP as drawn in Fig. 17: the thin dotted and solid lines are for $Z=0.004$ and $Z=0.05$, respectively; each dot along the lines show the age in step of 1 Gyr starting from 20 Gyr (top) down to 4 Gyr (bottom); the thin horizontal lines locate the loci of constant age (20, 15, 10, 7, and 5 Gyr starting from the top). Finally, the fading lines of SSP (in pairs because of the different metallicity) are shown for different values of the total mass, namely 10^{12} , 10^{11} , 10^{10} , 10^9 , and $10^8 \times M_\odot$ from right to left. The results are summarized in Table 7 limited to the group of galaxies that in Fig. 17 define the old age boundary. Incidentally, we note that in the case of M32 there is no contradiction between the median age of 8.5 Gyr estimated by Grillmair et al. (1996) looking at the distribution of stars in the CMD and the significantly younger age of $3.5 \div 4$ Gyr that we have adopted. This in fact corresponds to the youngest generation of stars in M32 whose traces are perhaps the brightest AGB stars in the CMD. If this young compo-

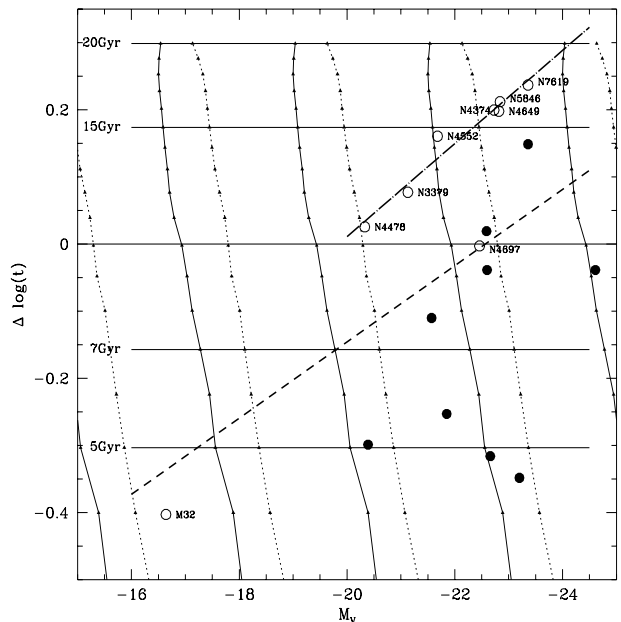


Fig. 17. The $\Delta \log(t)$ versus M_V relation. The *thick dashed line* is the linear regression of all the results. The *long-dashed dotted line* is the linear regression of the the data relative to the galaxies indicated by open circles (see the text for details). The position of M32, NGC 4649 and other *quiescent* galaxies (four of which are in the Virgo cluster) are indicated by the open symbols. Superposed to this diagram is the fading lines of SSPs: the thin dotted and solid lines are for $Z=0.004$ and $Z=0.05$, respectively; each dot along the lines show the age in step of 1 Gyr starting from 20 Gyr (top) down to 4 Gyr (bottom); the thin horizontal lines locate the loci of constant age (20, 15, 10, 7, and 5 Gyr starting from the top). Finally, the fading lines of SSP (in pairs because of the different metallicity) are shown for different values of the total mass, namely 10^{12} , 10^{11} , 10^{10} , 10^9 , and $10^8 \times M_\odot$ from right to left.

nent is really present it would dominate the contribution to H_β , whereas the old one would scarcely contribute to it. With this assumption for the zero point of the age scale, the oldest galaxies in the sample have the plausible age of $16 \div 17$ Gyr. In contrast, had we assumed the age of 8.5 Gyr as the zero point of our age scale, the age of the oldest galaxies would result unacceptably large (above 30 Gyr).

7. Isolation or mergers?

The fading lines in Fig. 17 help to visualize in the age-magnitude diagram the path followed by an evolving galaxy under a number of different scenarios. Perhaps the most intriguing question to address about galaxies is which of the two main avenues for their formation and evolution has prevailed as the dominant mechanism, i.e. isolation or mergers.

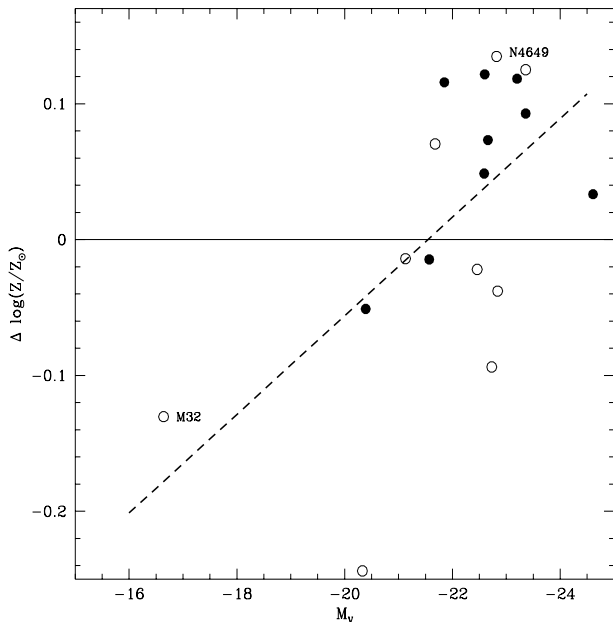


Fig. 18. The $\Delta \log(Z/Z_{\odot})$ versus M_V relation. The *thick dashed line* is the linear regression of the results. The position of M32, NGC 4649 and other *quiescent* galaxies (four of which are in the Virgo cluster) are indicated by the open symbols.

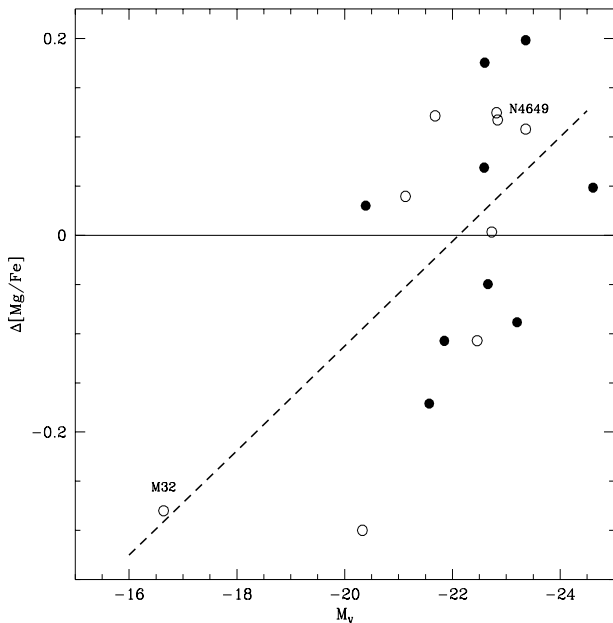


Fig. 19. The $\Delta[\text{Mg}/\text{Fe}]$ versus M_V relation. The *thick dashed line* is the linear regression of the results. The position of M32, NGC 4649 and other *quiescent* galaxies (four of which are in the Virgo cluster) are indicated by the open symbols.

Table 7. Estimated ages, metallicities, and enhancements of α -elements for the group of galaxies defining the old age edge in Fig. 17

NGC	Age	$\langle Z \rangle$	$[\text{Mg}/\text{Fe}]$
221	$3.5 \div 4.0$	0.0128	0.00
3379	$11 \div 12$	0.0167	0.22
4374	$15 \div 16$	0.0139	0.19
4478	$10 \div 11$	0.0098	-0.01
4552	$14 \div 15$	0.0202	0.40
4649	$15 \div 16$	0.0235	0.41
4697	$9 \div 10$	0.0164	0.18
5846	$13 \div 14$	0.0158	0.40
7619	$16 \div 17$	0.0230	0.39

If a galaxy forms and evolves in isolation, and suffers from a number of episodes of star formation (from one to several or even continuous) it would simply slide up and down along its fading line according to the stage of stellar activity at which the galaxy is detected with little transversal shift caused by chemical enrichment. Complicacies due to the possible presence of gas can be neglected here. As already said the data are compatible with this scheme suggesting that there are two groups of galaxies: those with no sign of rejuvenation in which either the overall duration or the epoch of the last episode of star formation seems to go inversely proportional to the galaxy mass, and those with signs of rejuvenation which are obviously scattered in this diagram.

The case of hierarchical merging is more difficult to discuss because the path is determined by the mass and evolutionary stage of the merging galaxies, and the amount of star formation taking place during the merger event. Let us suppose for the sake of simplicity that two identical units (same age, same composition, and say $10^{10} \times M_{\odot}$ mass each) merge triggering star formation in the composite system. The resulting galaxy will brighten by 0.75 magnitude because of the increased mass, shift to the line for the new total mass, slide down along this because of star formation, and slightly redden because of the increased metallicity (passing from $Z=0.001$ to $Z=0.05$ $\Delta M_V = 1.0$ magnitudes at most). The total displacement vector depends on the relative amount of gas turned into stars. In any case, the displacement will be nearly vertical along the $2 \times 10^{10} M_{\odot}$ line in our example. As soon as star formation is over, the galaxy will fade at slowing rate back to a point near to the original position ($M_V - 0.75$). It is worth recalling that the recovery time after a burst of stellar activity is short (going from a few 10^8 yr to 1 Gyr at most. In principle there is no contradiction between this

scenario and the bunch of galaxies scattered in this diagram toward much younger ages. The problem is with they recovering position if this latter corresponds to the group of galaxies with no sign of rejuvenation. Indeed if the seed galaxies had the same age we would expected the daughter galaxies to cluster along a nearly horizontal line in this diagram. In contrast, it seems as if bright, high mass galaxies had their merger adventure long ago, whereas the faint, low mass objects did it in a more recent past, but starting from seed galaxies with small stellar content. This is equivalently to say that the bulk of star forming activity took place more and more toward the present at decreasing mass of the galaxy. Furthermore, *why do not we see in this diagram any low mass galaxy (the potential seeds of a bigger galaxy in the hierarchical scheme) at the same age range of the big galaxies ? Is this only due to selection effects in our sample (because no dwarf galaxies but M32 are present) or more subtle causes are to be considered?* As nowadays answering this question is difficult owing to the lack of sufficient data with precise measurements of H_β , Mg_2 and $\langle Fe \rangle$.

8. SN-driven winds or variable IMF?

To explain the color-magnitude relation (CMR) of early type galaxies (cf. Bower et al. 1992 for the case of the Virgo and Coma galaxies), long ago Larson (1974) postulated that it is the consequence of SN-driven galactic winds. In the classical scenario, isolation and constant IMF, massive galaxies eject their gaseous content much later and get higher mean metallicities than the low mass ones. The implication is that the global duration of the star forming activity is proportional to the galaxy mass, contrary to what required by the simplest interpretation of the α -enhancement problem (cf. Matteucci 1997 for a recent review of the subject). The present analysis seems to confirm that on the average more luminous galaxies are more enhanced in α -elements. The trend holds for those with no sign of rejuvenation (cf. Fig. 19) at least as it stems from comparing NGC 4478 to the remaining galaxies in this group. The situation is less clear for the others. However, taken as face values, the results of our analysis weaken the classical SN-driven wind model. Furthermore, the CMR requires that more massive galaxies are indeed more metal-rich than the low mass ones. The alternative that the CMR can be understood as an age sequence in the sense that blue galaxies have started star formation much later than in red ones has been proved to disagree with the redshift evolution of early type galaxies in the HST Deep Field (cf. Kodama & Arimoto 1996). As examined in the previous section the merger scenario has some intrinsic difficulties with the distribution of galaxies in the age-luminosity plane, and perhaps the predictions for the narrow band indices and chemical properties (cf. the experiment made with Model-C).

It follows from all this that the only viable solution of the puzzle is a scheme in which all galaxies have begun to form stars at the same time but, depending on their mass, the process has continued (maybe in discrete episodes) over different periods of time. Massive galaxies did it in the far past, the star forming period ceased very soon, the material has been significantly enriched in metals and α -elements. Low mass galaxies started at the same epoch, but continued for longer periods of time (the duration increasing at decreasing galactic mass), got less metal enriched and α -enhanced (for global periods of star formation longer than about 1 Gyr this is less of a problem).

Can such a scheme result from standard assumptions concerning star formation and IMF? The answer is not. In a recent paper Chiosi et al. (1997) have proposed new models of elliptical galaxies in which the IMF instead of being constant is a function of density, temperature and velocity dispersion of the medium in which stars are formed (cf. Padoan et al. 1997). In brief, in a hot, rarefied medium the new IMF is more skewed towards the high mass end than in a cool, dense medium. This kind of situation is met passing from a high mass (low mean density) to a low mass (high mean density) galaxy or from the center to the periphery of a given galaxy. The above dependence of the IMF yield galactic models having the desired behaviour, thus providing a plausible way out to the above points of contradiction encountered with the standard scheme. These models in fact predict the onset of galactic winds and consequent termination of the star forming period much earlier in massive galaxies than in the low mass ones. The reason of it resides in the skewness of the IMF toward the high mass end that changes with the mean gas density (galactic mass and/or position within a galaxy) thus favoring in massive galaxies the relative percentage of SN explosions and consequent heating of the gas to the escape velocity. In this scheme massive galaxies despite their short duration of stellar activity yet reach high metallicities and $[Mg/Fe]$ ratios. The opposite occurs in the low mass ones. See Chiosi et al. (1997) for all details. Finally, we notice that the results of the variable IMF scheme are also compatible with the indications arising from the present study, in particular the age ranking inferred from H_β .

9. Conclusions

In this study we have thoroughly investigated the ability of the H_β , Mg_2 and $\langle Fe \rangle$ diagnostic to assess chemical abundances and their ratios and ages of elliptical galaxies. In particular we have addressed the question whether different slopes of the gradients in Mg_2 and $\langle Fe \rangle$ across galaxies do automatically imply an enhancement of the $[Mg/Fe]$ ratio. Second, we have tackled the problem of the real information hidden in the different values of H_β , Mg_2 and $\langle Fe \rangle$ observed in the nuclear regions of elliptical

galaxies. The results of this study can be summarized as follows:

1. The Line strength indices Mg_2 and $\langle Fe \rangle$ do not simply correlate with the chemical abundances. To infer from line strength indices the corresponding chemical abundances (and their ratios) one needs to know: (i) the star formation history of the galaxy; (ii) the metallicity partition function $N(Z)$; (iii) and via a suitable calibration the effects of the enhancement in α -elements on the line strength indices. This conclusion does not depend on the particular models and calibration used to perform our experiments, but stems from the intrinsic properties of the line strength indices themselves.
2. We provide basic calibrations for the variations δH_β , δMg_2 and $\delta \langle Fe \rangle$ as a function of age $\Delta \log(t)$ (in Gyr), metallicity $\Delta \log(Z/Z_\odot)$, and $\Delta[Mg/Fe]$ of SSPs whose application is of general use.
3. Limited to three galaxies of the Carollo & Danziger (1994a,b) catalog we analyze the implications of the gradients in Mg_2 and $\langle Fe \rangle$ observed across these systems. It is shown from a qualitative point of view how the difference δMg_2 and $\delta \langle Fe \rangle$ between the values of each index at any radial distance with respect to their central values would translate into the $\Delta[Mg/Fe]$, $\Delta \log(Z/Z_\odot)$, and $\Delta \log(t)$ differences between the local and the central values.
4. The above calibration is used to explore the variation from galaxy to galaxy of the nuclear values of H_β , Mg_2 , and $\langle Fe \rangle$ limited to a sub-sample of the Gonzales (1993) catalog. The differences δH_β , δMg_2 , and $\delta \langle Fe \rangle$ are converted into the differences $\Delta \log(t)$, $\Delta \log(Z/Z_\odot)$, and $\Delta[Mg/Fe]$. Various correlations among the age, metallicity, and enhancement variations are explored. In particular we thoroughly examine the relationships $\Delta \log(t) - M_V$, $\Delta \log(Z/Z_\odot) - M_V$, and $\Delta[Mg/Fe] - M_V$, and advance the suggestion that the duration of the star formation period gets longer or the last episode of stellar activity gets closer and closer toward the present at decreasing galaxy mass. This result is discussed at the light of predictions from the merger and isolation models of galaxy formation and evolution. In brief, we conclude that none of these can explain the results of our analysis, and suggest that the kind of time and space dependent IMF proposed by Padoan et al. (1997) and the associated models of elliptical galaxies elaborated by Chiosi et al. (1997) should be at work.

This study has been financed by the Italian Ministry of University, Scientific Research and Technology (MURST), the Italian Space Agency (ASI), and the TMR grant ERBFMRX-CT96-0086 from the European Community.

References

Arimoto N., Yoshii Y. 1987, A&A 173, 23

- Barbuy B. 1994, ApJ 430, 218
 Bertelli G., Bressan A., Chiosi C., Fagotto F., Nasi E. 1994, A&AS 106, 275
 Bertin G., Saglia R.P., Stiavelli M. 1992, ApJ 384, 423
 Borges A.C., Idiart T.P., De Freitas Pacheco J.A., Thevenin F. 1995, AJ 110, 2408
 Bower R.G., Lucey J.R., Ellis R.S. 1992, MNRAS 254, 589
 Bressan A., Chiosi C., Fagotto F. 1994, ApJS 94, 63
 Bressan A., Chiosi C., Tantalo R. 1996, A&A 311, 425
 Burstein D., Bertola F., Buson L.M., Faber S.M., Lauer T.R. 1988, ApJ 328, 440
 Carollo C.M., Danziger I.J., Buson L. 1993, MNRAS 265, 553
 Carollo C.M., Danziger I.J. 1994a, MNRAS 270, 523
 Carollo C.M., Danziger I.J. 1994b, MNRAS 270, 743
 Carraro G., Lia C., Chiosi C. 1997, MNRAS, submitted
 Chiosi C., Bressan A., Portinari L., Tantalo R. 1997, A&A submitted
 Davidge T.J., Jones J.H. 1992, AJ 104, 1365
 Elston R., Silva D.R. 1992, AJ 104, 1360
 Faber S.M., Worthey G., Gonzales J.J. 1992, in IAU Symp. 149, B. Barbuy and A. Renzini (eds.), p.255
 Freedman W.L. 1989, AJ 98, 1285
 Freedman W.L. 1992, AJ 104, 1349
 Gibson B.K. 1996, MNRAS, submitted
 Gibson B.K. 1994, MNRAS 271, L35
 Gonzales J.J. 1993, Ph.D. Thesis, Univ. California, Santa Cruz
 Grillmair C.J., Lauer T.R., Worthey G., et al. 1996, AJ 112, 1975
 Hardy E., Couture J., Couture C., Joncas G. 1994, AJ 107, 195
 Idiart T.P., de Freitas Pacheco J.A. 1995, AJ 109, 2218
 Kodama T., Arimoto N. 1997, A&A in press
 Larson R.B. 1974, MNRAS 166, 585
 Matteucci F. 1997, Fund. Cosmic Phys. in press
 O'Connell R.M. 1988, in Starbursts and Galaxy Evolution, ed. T.X. Thuan, T. Montmerle, & J. Tran Than Van p. 367. Gif-sur Yvette: Editions Frontieres.
 Padoan P., Nordlund A.P., Jones B.J.T. 1997, preprint
 Portinari L., Chiosi C., Bressan A. 1997, A&A to be submitted
 Schweizer F., Seitzer P. 1992, AJ 104, 1039
 Tantalo R., Chiosi C., Bressan A. 1997, A&A, to be submitted
 Tantalo R., Chiosi C., Bressan A., Fagotto F. 1996, A&A 311, 361
 Thielemann F.K., Nomoto K., Hashimoto M. 1993, in *The Origin and Evolution of Elements*, ed. N. Prantzos et al. p. 297, Cambridge: Cambridge Univ. Press
 Thielemann F.K., Nomoto K., Hashimoto M. 1996, ApJ 460, 408
 Weiss A., Peletier R.F., Matteucci F. 1995, A&A 296, 73
 Worthey G. 1992, Ph.D. Thesis, Univ. California, Santa Cruz
 Worthey G., Faber S.M., Gonzales J.J., Burstein D. 1994, ApJS 94, 687
 Young P.J. 1976, AJ 81, 807

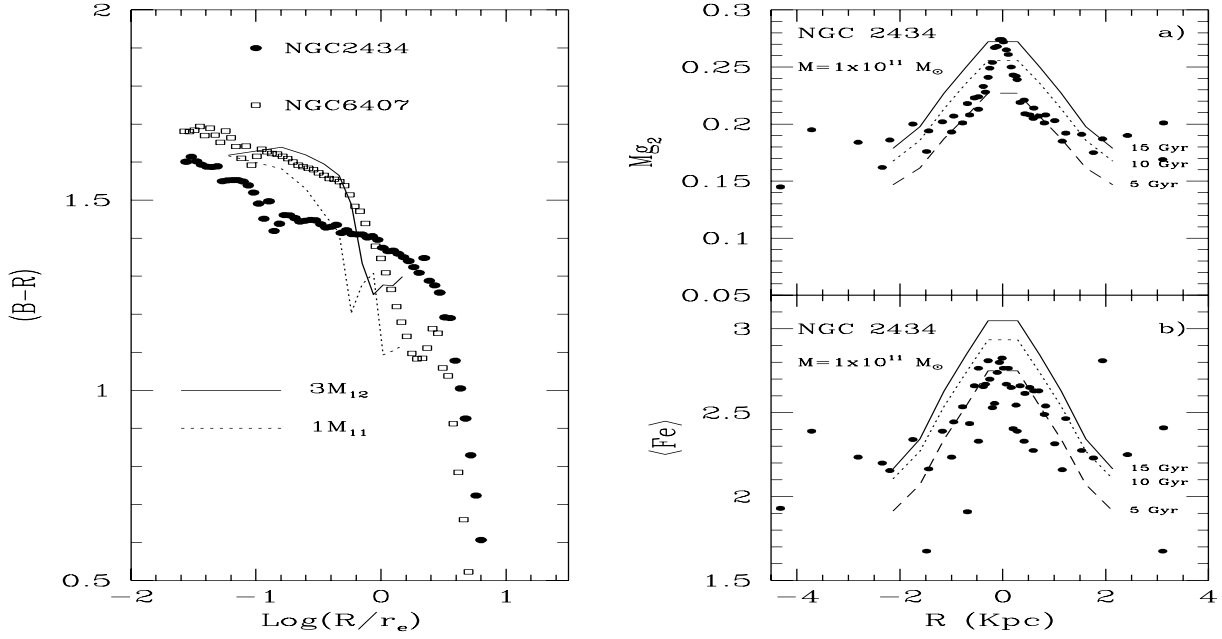


Fig. 1. Gradients in colors and line strength indices for the galaxies NGC 2434 and NGC 6407 (Carollo & Danziger 1994a), filled and open circles, respectively. *Left Panel:* comparison with the theoretical gradients in $(B-R)$ for models of different mass and same age (15 Gyr). *Right Panel:* comparison with the theoretical gradients in line strength indices for the $1 \times 10^{11} M_{\odot}$ model which has nearly the same M/L_B ratio as NGC 2434.

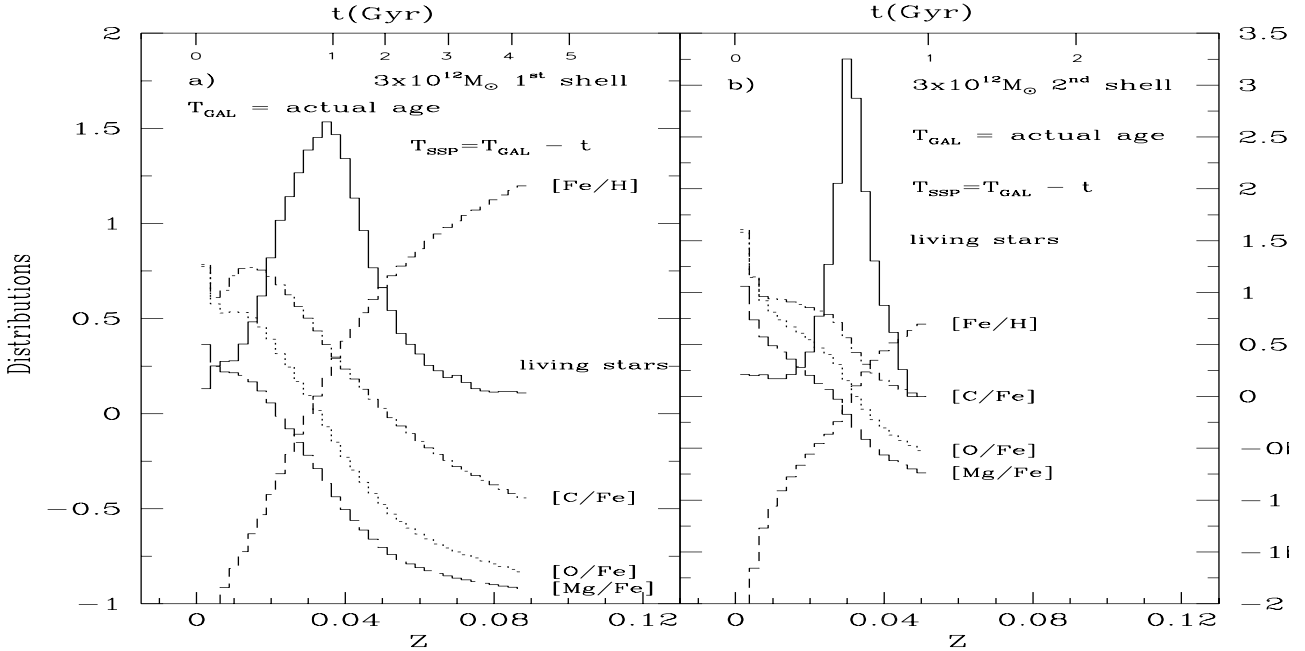


Fig. 3. Panels (a) and (b): the number of living stars and abundance ratio distribution per metallicity bin in the 1st and the 2nd shells, respectively, of the galaxy with mass ($3 \times 10^{12} M_{\odot}$). The abundance ratios are in the standard notation. The *solid line* is distribution of living stars in units of $10^{11} \times M_{\odot}$. The *dotted, dashed, long-dashed, and dot-dashed* lines give the distribution per metallicity bin of $[O/Fe]$, $[Fe/H]$, $[Mg/Fe]$ and $[C/Fe]$, respectively. The top scale gives the birth-time $t = T_G - T_{SSP}$ in Gyr of a SSP of age T_{SSP} in a galaxy of age T_G .